3-10-2011

Phonons of single quintuple Bi2Te3 and Bi2Se3 films and bulk materials

Wei Cheng
Illinois State University

Shang-Fen Ren
Illinois State University

Phonons of single quintuple Bi_2Te_3 and Bi_2Se_3 films and bulk materials

Wei Cheng
College of Nuclear Science and Technology, Beijing Normal University, Beijing 100875, People's Republic of China

Shang-Fen Ren
Department of Physics, Illinois State University, Normal, Illinois 61761, USA

(Received 5 October 2010; revised manuscript received 11 January 2011; published 10 March 2011)

Phonons of single quintuple films of Bi_2Te_3 and Bi_2Se_3 and corresponding bulk materials are calculated in detail by MedeA (a trademark of Materials Design) and Vienna *ab initio* simulation package (VASP). The calculated results with and without spin-orbit couplings are compared, and the important roles that the spin-orbit coupling plays in these materials are discussed. A symmetry breaking caused by the anharmonic potentials around Bi atoms in the single quintuple films is identified and discussed. The observed Raman intensity features in Bi_2Te_3 and Bi_2Se_3 quintuple films are explained.

DOI: 10.1103/PhysRevB.83.094301 PACS number(s): 68.55.ag, 63.20.dk, 63.22.Dc, 78.30.Fs

I. INTRODUCTION

Bi_2Te_3 and Bi_2Se_3 are the best known bulk thermoelectric materials today.[1–7] Recently, they have also been demonstrated to be topological insulators, i.e., insulators with conductive surface states shaped in a Dirac cone that are robustly protected against any time-reversal perturbation, such as crystal defects and nonmagnetic impurities.[8–14] These topological insulators are attractive for both fundamental research and for potential applications in spintronics, quantum computing, magnetic memory, low-energy dissipation electronics, etc. Because of the broad range of promising potential applications, research attention on these materials has increased dramatically in recent years.[8–21]

Single-crystal Bi_2Te_3 and Bi_2Se_3 have the same rhombohedral crystal structure, with five atoms in one unit cell. Their atomic arrangement is a layered structure, with each layer consisting of five monoatomic planes of -Te(Se)-Bi-Te(Se)-Bi-Te (Se) (see Fig. 1); each of these five atomic planes is referred to as a quintuple layer (QL). The QLs are weakly bound to each other by the van der Waals forces. Thin films with a few QLs are almost two-dimensional (2D) semiconductors, and the confinement of phonons in the growth direction, or the *c* axis, of the films could greatly enhance the figure of merit of the films.[19,20,22,23] These films are also particularly promising for investigating the unique physical properties and potential practical applications of topological insulators.

Experimentally, several successful methods of creating very thin films with only a few QLs have been reported, such as mechanically peeling off single QL films of Bi_2Te_3 from the bulk,[15,16,19–21] directly growing a few-QL nanoplates,[17] and controlled mechanical exfoliation of Bi_2Se_3 by an atomic force microscope (AFM) to a few QLs.[18]

The Raman spectra of a few-QL films of Bi_2Te_3 (Refs. 15, 16, 19–21) and Bi_2Se_3 (Ref. 24) have been reported. It has been found that the Raman peak positions are almost the same as those of the corresponding bulk materials, and there is one extra A_{1u} peak[25,26] [the A_{2u} modes in the MedeA[25,26] notation used in our calculations are their A_{1u} modes]. It has also been found that the intensity ratios of the out-of-plane A_{1u} and A_{1g} modes to the in-plane E_g modes grow with decreasing film thickness.[16] Clearly there are symmetry breakings in the thin films that result in the Raman activity of the A_{1u} mode that is not Raman active in bulk materials.

Even though several Raman experimental research studies have reported on Bi_2Te_3 and Bi_2Se_3 thin films, the theoretical investigations on the phonon properties of these films are lacking. To our knowledge, there are existing calculations on the lattice dynamics and thermal conductivity of the bulk materials with the empirical force field model and molecular-dynamic simulations,[27–29] but there are no *ab initio* calculations with spin-orbit coupling (SO) included. In order to understand the important roles that SO plays in the phonon properties of these materials, and the differences between the phonons in the QL thin films and in corresponding bulk materials, we have carried out a detailed investigation on phonons of single QL films of Bi_2Te_3 and Bi_2Se_3 with five atomic layers as well as phonons of the corresponding bulk materials. The calculated results are analyzed, and the important roles that SO plays in these materials are discussed. The calculated results are also compared with the experimental measurement, and the observed Raman intensity features in Bi_2Te_3 and Bi_2Se_3 quintuple films are explained.

This paper is organized in the following manner: In Sec. II, we will discuss our computational details, including the structures of the materials and the comparison of two theoretical approximations. In Sec. III, we will show our calculated results and analyze those results. We will discuss the phonon results calculated with and without SO for both the bulk materials and the quintuple films, phonon dispersions of the materials under different pressures, the splitting of degenerate phonon modes at the Γ point owing to anharmonic potentials, and the Raman spectra in films and bulk materials. Section IV is the conculsion.

II. COMPUTATIONAL DETAILS

A. Structures of the bulk materials and the single quintuple layer films

The structures of the bulk materials and the single QL films are shown in Fig. 1. In Fig. 1(a), three QLs are shown in the unit cell in the bulk materials, and the primitive unit cell of the bulk material is also shown. The unit cell of the single QL films

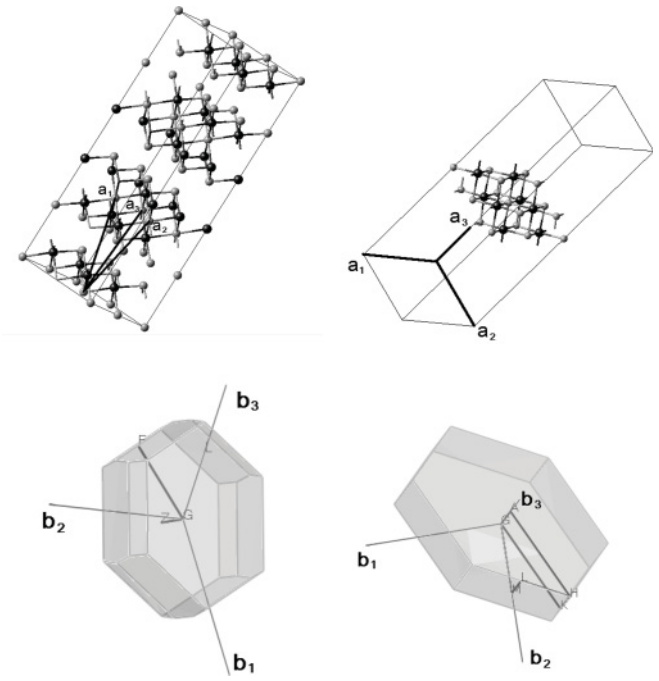

FIG. 1. Structures of Bi_2Te_3 (or Bi_2Se_3) bulk and thin film (top) and their corresponding Brillouin zone (bottom), where (a) is for bulk and (b) is for film. The black balls are Bi atoms, and the gray balls are Te (or Se) atoms. In the above figures, a_1,a_2,a_3 are the translational vectors in the real space, and b_1,b_2,b_3 are the reciprocal lattice vectors derived from them. The gray lines show the Brillouin zone. Here L is $(0\frac{1}{2}0)$ and Z is $(\frac{1}{2}\frac{1}{2}\frac{1}{2})$ in the corresponding reciprocal coordinate systems.

is shown in Fig. 1(b), and in our calculations is taken as the following: We delete two QLs from the bulk unit cell as shown in Fig. 1(a), and enlarge the structure in the perpendicular direction, which is defined as the z direction. This means that vacuum is introduced in the unit cell other than the single QL. We then optimize the atom positions and cell lengths to get a minimum energy structure [shown in Fig. 1(b)]. The finalized structural details in our calculations, including the period in the z direction, or the lattice constant of c, for these single QL films as well as corresponding bulk materials, are listed in Table I. We can see that for the single QL structures of both the Bi_2Te_3 and Bi_2Se_3, the periods in the z direction are more than 3 nm, and the van der Waals interactions in this range are very weak, so the van der Waals interactions among QLs in Fig. 1(b) are very weak compared to those in Fig. 1(a). Because of the structure differences, the phonon properties in the single QL films and in corresponding bulk materials should be different. The single QL films and the bulk materials have different symmetries. The film has P-3m1 symmetry, and the bulk has R-3m symmetry. Also, because of its limited thickness, the films have no translational symmetry in the third dimension. Therefore, the first symmetry breaking from the bulk materials to its single QL films is the decrease of translational symmetry in films. However, the irreducible representation of the phonon modes of the two structures remains the same.

In our calculations, the supercell of the bulk materials includes 15 atoms, which is three times the primitive unit cell of the bulk materials [1/4 of the cell shown in Fig. 1(a)], and the supercell of single QL films includes 20 atoms [shown in Fig. 1(b)], which includes four primitive unit cells of the film.

For convenience, we present Fig. 2 here, which is the same as Fig. 3(b) in Ref. 16 and Fig. 2 in Ref. 27 for bulk materials.[16,27] From this figure, it is shown that in the bulk materials the A modes are mainly vibrations along the growth direction and the E modes are mainly coupled vibrations within the QLs.

B. Comparison of the local-density and generalized gradient approximations

The phonons of the film as well as of the bulk are calculated by the MedeA-VASP,[25,26] with and without SO. Electronic structures are calculated by density-functional theory.[5] The calculations are carried out with two approximations, the local-density approximation (LDA)[30,31] and the generalized gradient approximation (GGA).[32–34] It is found in our calculations that the LDA underestimates and the GGA overestimates the lattice constants. The comparisons of the calculated results of LDA and GGA are listed in the first two columns of Table I. In general, our results agree well with other published calculations[5] using these software packages. Because of this, LDA overestimates and GGA underestimates the phonon frequencies. In the rest of this paper, the phonon calculations are carried out in the framework of the Perdew-Burke-Ernzerhof generalized gradient approximation (GGA-PBE) of the density functional.[32–34] We chose it because the calculated results agree best with the experimental data. The cutoff frequencies are chosen to be 460 eV. The convergences of phonon frequencies for both of the films and the bulks are tested. It is found that the k points of $5 \times 5 \times 1$ and $7 \times 7 \times 3$ for films produce almost the same phonon dispersion and phonon frequencies for films. For example, the highest phonon frequency calculated by a $5 \times 5 \times 1$ k point for the Bi_2Te_3 quintuple film (GGA) is 4.200, and the frequency calculated by a $7 \times 7 \times 3$ k point is 4.176. The computational intensity of the latter is almost six times of the first one, but the calculated number difference is less than 0.6%. Because of this, we used $5 \times 5 \times 1$ for other film calculations. For bulk materials, we used the k point of $11 \times 11 \times 11$, which is enough to get good phonon dispersion for corresponding bulk materials (a bigger unit cell requires less k points because the bigger unit cell in real space corresponds to a smaller unit cell in reciprocal space).

III. RESULTS AND DISCUSSIONS

We have carried out detailed calculations of phonons in Bi_2Te_3 and Bi_2Se_3 single QL films with five atomic layers and in the corresponding bulk materials, with and without SO. The computation details, the optimized structures, and the calculated phonon frequencies at the Γ point are all listed in Table I. The phonon dispersions of bulk Bi_2Se_3 with and without SO are shown in Fig. 3, and the phonon dispersions of a single QL of Bi_2Te_3 and Bi_2Se_3 with and without SO are shown

TABLE I. Calculation details of the optimized single QL films and corresponding bulks without and with spin-orbit interactions (SO). The cutoff energy is taken as 460 eV and the structure angles are all taken as $90^\circ \times 90^\circ \times 120^\circ$ in all of these calculations. The frequencies shown are frequencies at the Γ point. The unit of frequency is THz. (a) denotes low-frequency modes and (b) denotes high-frequency modes. The Raman- or infrared-active modes according to the group theory are indicated by R or I. Raman-measured data are shown in brackets. The numbers in parentheses are the experimental values from Ref. 16 for Bi_2Te_3 film and bulk, from Ref. 24 for Bi_2Se_3 film, and from Ref. 27 for Bi_2Se_3 bulk.

Materials	Bi_2Se_3 (bulk)	Bi_2Se_3 (bulk)	Bi_2Se_3 (film)	Bi_2Te_3 (bulk)	Bi_2Te_3 (film)	Bi_2Se_3 (bulk)	Bi_2Se_3 (film)	Bi_2Te_3 (bulk)	Bi_2Te_3 (film)
Approximations	LDA, SO	GGA, SO	GGA, SO	GGA, SO	GGA, SO	GGA	GGA	GGA	GGA
k points	$11 \times 11 \times 11$	$11 \times 11 \times 11$	$5 \times 5 \times 1$	$11 \times 11 \times 11$	$5 \times 5 \times 1$	$11 \times 11 \times 11$	$5 \times 5 \times 1$	$11 \times 11 \times 11$	$7 \times 7 \times 3$
3D supercell lattice constant a,c (nm)	0.411 753 2.773 224	0.421 534 2.982 863	0.839 560 5.802 452	0.447 341 3.112 834	0.888 157 3.704 437	0.413 800 2.864 000	0.836 811 8 3.468 198 8	0.445 000 3.163 000	0.885 979 7 3.694 066 4
VASP free energy (eV)	−24.782 186	−21.886 519	−87.444 172	−20.481 879	−81.610 305	−20.416 524	−81.943 300	−18.709 863	−74.674 817
E_u (I)	−0.085	0.063	−0.231,0.058	0.044	−0.147, − 0.114	−0.025	0.032,0.036	−0.021	−0.069,0.033
A_{2u} (I)	−0.151	−0.105	0.076	−0.052	−0.069	−0.038	−0.016	−0.124	−0.088
$E_{g(a)}$ (R)	1.244	1.166	1.15,1.173	1.063(1.03)	0.894,0.901(1.17)	1.263	1.118,1.328	1.090(1.03)	1.004,1.02(1.17)
$A_{1g(a)}$ (R)	2.261	1.914	1.814	1.615(1.86)	1.512(1.83)	2.236	1.818	1.616(1.86)	1.484(1.83)
$E_{u(a)}$ (I)	2.407	1.939	2.032,2.073	1.451	1.567,1.571	2.550	2.285,2.323	1.893	1.935,1.943
$E_{u(b)}$ (I)	3.913	3.802	3.763,3.765	2.735	2.802,2.804	3.986	3.772,3.824	2.920	2.927,2.932
$E_{g(b)}$ (R)	4.109	3.717	3.616,3.626(3.93)	2.876(3.05)	2.873,2.878(3.04)	4.164	3.882,3.936(3.93)	3.130(3.05)	3.071,3.084(3.04)
$A_{2u(a)}$ (I)	4.116	4.098	4.342	2.850	3.199(3.50)	4.279	4.449	3.075	3.275(3.50)
$A_{2u(b)}$ (I)	4.837	4.660	4.97	3.556	3.973	5.010	5.121	3.844	4.098
$A_{1g(b)}$ (R)	5.127(4.95)	4.987(4.95)	5.074(5.22)	3.814(4.02)	4.092(3.98)	5.380(4.95)	5.242(5.22)	4.114(4.02)	4.176(3.98)

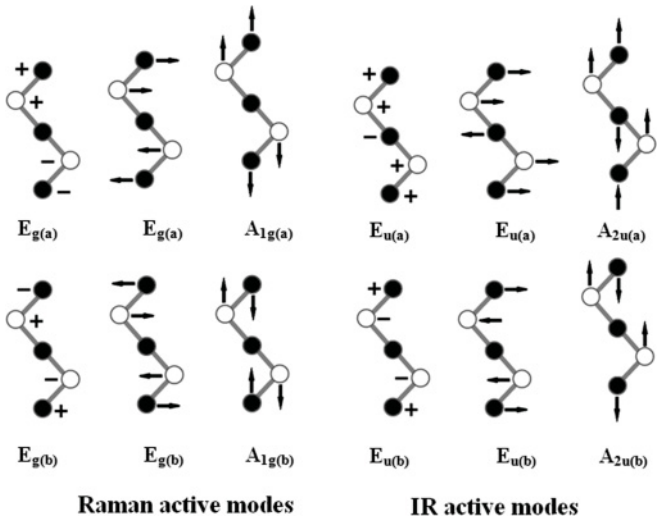

FIG. 2. (Color online) The irreducible representations of vibrational modes of bulk Bi_2Se_3 or Bi_2Te_3 taken from Ref. 27. From this figure, we can see that the *A* modes are mainly perpendicular to the films and and the *E* modes are mainly within the films.

in Figs. 4 and 5. The phonon dispersions with different pressure are shown in Fig. 6, and the effects of anharmonic potentials are shown in Fig. 7. Next we will discuss the important findings in these results in detail.

A. Spin-orbit coupling effect

In our calculations, we found that not only is SO important to produce good electronic band structures, but it is also important in calculating phonon properties accurately in these materials. The calculated frequencies with and without SO can be quite different. The optimized structure of bulk Bi_2Se_3 and Bi_2Te_3 with SO is obtained by MedeA calculations. These calculations are very time consuming and also take a huge amount of computer memory. In our calculations, we found that both GGA and LDA results indicate that the SO leads

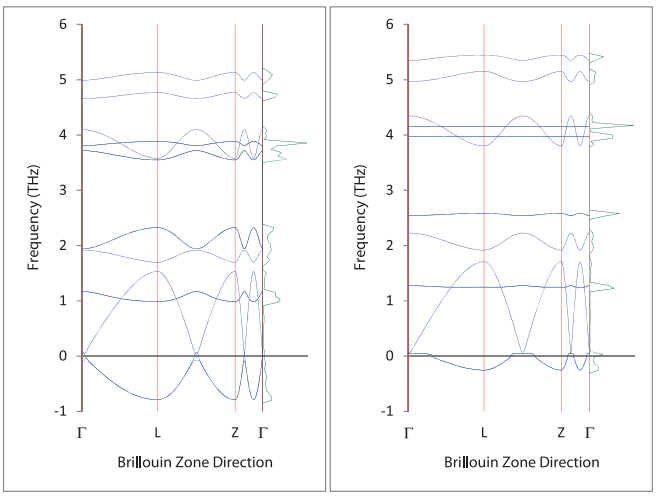

(a) (b)

FIG. 3. (Color online) Phonon dispersions of bulk Bi_2Se_3 (a) with SO and (b) without SO. Here *L* stands for $(0\frac{1}{2}0)$ and *Z* stands for $(\frac{1}{2}\frac{1}{2}\frac{1}{2})$ in the trigonal coordinate system.

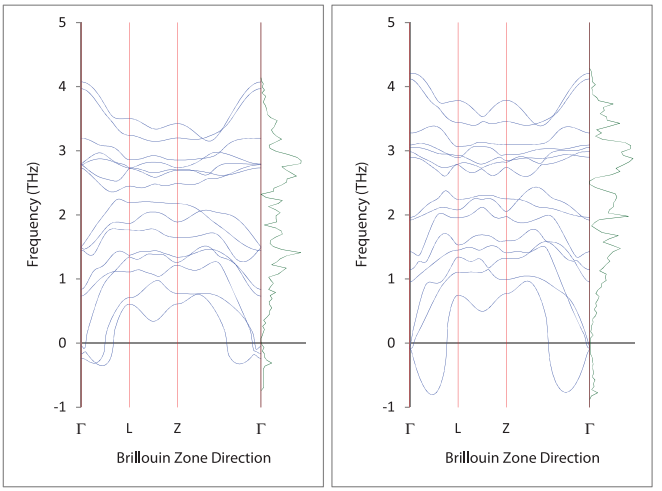

(a) (b)

FIG. 4. (Color online) Phonon dispersion of Bi_2Te_3 film with anharmonic interactions (a) with SO and (b) without SO. Here *L* stands for $(0\frac{1}{2}0)$ and *Z* stands for $(\frac{1}{2}\frac{1}{2}\frac{1}{2})$ in the hexagonal coordinate system.

to larger lattice constants and lower phonon frequencies for both bulks and films, which agree better with experimental measurements. For example, the highest frequency of an optimized bulk Bi_2Se_3 structure using LDA and including SO is 5.127 THz, and the highest frequency of an optimized bulk Bi_2Se_3 structure using GGA and including SO is 4.987 THz. The highest frequency using GGA without SO is 5.380 THz. The experimental value of bulk Bi_2Se_3 is close to 4.95 THz.[27]

The importance of SO will be discussed in more detail later. In our calculations we have found that the VASP energy with SO is ∼1.5 eV lower than that without SO, so we know that SO is also important for free-energy calculation in the QL systems. Because of the importance of SO, we will include SO to analyze phonon properties later.

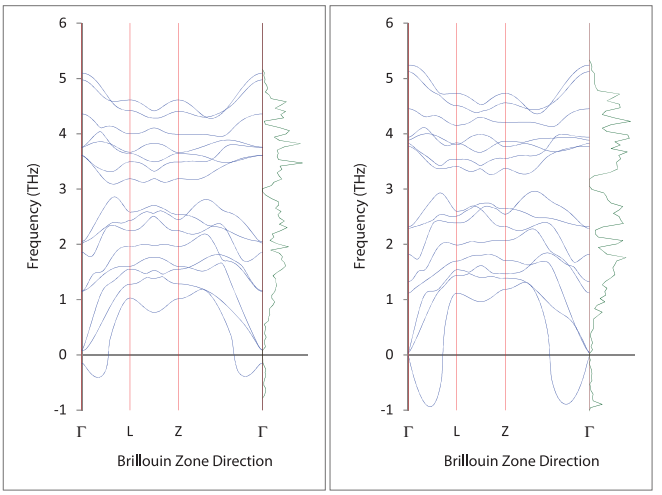

(a) (b)

FIG. 5. (Color online) Phonon dispersion of Bi_2Se_3 film with anharmonic interactions (a) with SO and (b) without SO. Here *L* stands for $(0\frac{1}{2}0)$ and *Z* stands for $(\frac{1}{2}\frac{1}{2}\frac{1}{2})$ in the hexagonal coordinate system.

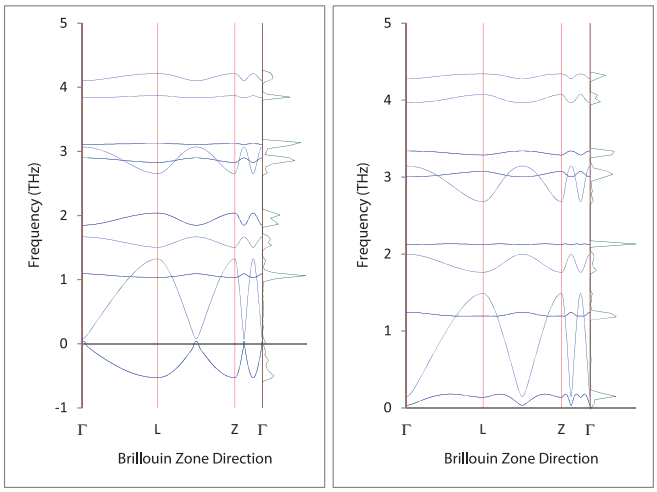

(a) (b)

FIG. 6. (Color online) Phonon dispersion of two bulk Bi_2Te_3 structures with different pressures. The VASP energies are −18.709 566 eV for (a) and −18.639 107 eV for (b). Electronic pressures are 53.000 MPa for (a) and 2.066 GPa for (b). Here L stands for $(0\frac{1}{2}0)$ and Z stands for $(\frac{1}{2}\frac{1}{2}\frac{1}{2})$ in the trigonal coordinate system.

B. Phonon eigenmodes of bulk materials with and without SO

The phonon dispersions of bulk Bi_2Se_3 with and without SO calculated by GGA are shown in Fig. 3. The QL normal is in [111] direction in the trigonal coordinate systems, as shown in Fig. 1. The symbols in the dispersion of Fig. 3 stand for $\Gamma[000]$, $L[0\ \frac{1}{2}\ 0]$, and $Z[\frac{1}{2}\frac{1}{2}\frac{1}{2}]$, as shown in Fig. 1. The first thing we can easily see from Fig. 3 is that there are three nontrivial parts in the ΓZ direction and two nontrivial parts in the LZ direction in the reciprocal lattice. This is because the unit cell of the bulk materials shown in Fig. 1 contains three QLs.

From Fig. 3, we can see that when phonon dispersion of bulk Bi_2Se_3 is calculated without SO [as shown in Fig. 3(b)],

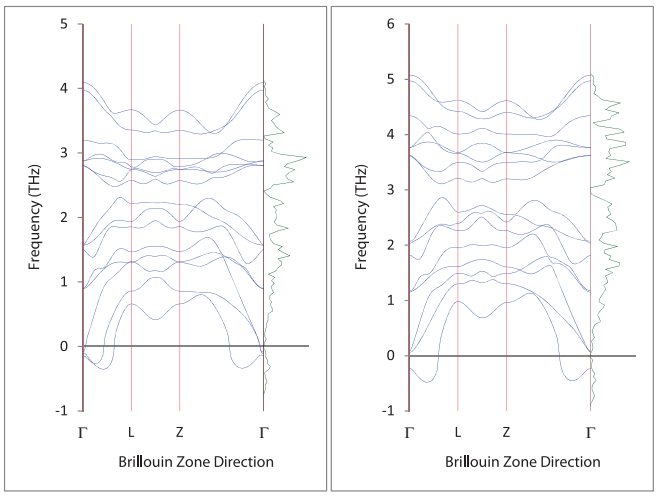

(a) (b)

FIG. 7. (Color online) Phonon dispersion of (a) Bi_2Te_3 and (b) Bi_2Se_3 film with harmonic interactions and SO. Here L stands for $(0\frac{1}{2}0)$ and Z stands for $(\frac{1}{2}\frac{1}{2}\frac{1}{2})$ in the hexagonal coordinate system.

four branches with Γ-point frequencies at 4.164, 3.986, 2.550, and 1.263 THz are almost dispersionless. Comparing these frequencies with the irreducible representations in Table I, we can see that all of these branches correspond to E modes. This tells us that all of the optical E branches of Bi_2Se_3 bulk materials are quite flat without SO, which means that these E modes are all mainly localized within the QL of the bulk materials when the SO is not considered. However, when SO is included in the phonon calculations, as shown in Fig. 3(a), the QLs interact with each other and the E modes propagate between layers. The difference between Figs. 3(a) and 3(b) tells us that it makes critical differences in the phonon properties of Bi_2Se_3 to include SO, because SO provides an extra atom-atom potential to correct the flat dispersion in Fig. 3(b).

From Figs. 2 and 3 and Table I, we conclude that SO is more important to modes with in-plane vibrations. This is a unique property of QL crystals such as Bi_2Te_3 and Bi_2Se_3 that does not exist in other semiconductor materials that we have studied previously.[35]

Next, we will analyze the phonon eigenmodes of bulk Bi_2Se_3 one by one, and compare those calculated with SO [Fig. 3(a)] and those calculated without SO [Fig. 3(b)].

The highest-frequency mode with a calculated frequency of 4.987 THz in Fig. 3(a) is Raman-active A_{1g} mode (the Raman data is 4.95 THz). The vibration direction of this mode is perpendicular to the QL. The next two high-frequency modes of 4.660 and 4.098 THz are Raman-inactive A_{2u} modes. Our studies show that the frequencies of these two modes are sensitive to the van der Waals interaction between QLs, and they are also mainly from out-of-plane vibrations. These three A modes, one A_{1g} and two A_{2u}, and the dispersion of these three A modes, are not affected much by the SO. They are also not affected much by the anharmonic potentials, which will be discussed later.

The next two modes in Fig. 3(a) are the E_g (3.802 THz) and E_u (3.717 THz) modes, corresponding to the two almost dispersionless branches in Fig. 3(b). These two modes are split by the van der Waals interactions. In general, we know from Fig. 2 that the vibrations of both E_g and E_u are mainly within the plane. These modes should have the same frequencies in an isolated plane with the same E irreducible representations. However, because the van der Waals interactions between planes are coupled with the in-plane vibrations, these two degenerated frequencies split, but still correspond to two close frequencies. By comparing Figs. 3(a) and 3(b), we can see that the SO effect is significant for these two branches.

The next two modes at 1.939 and 1.914 THz, almost degenerating at the Γ point as shown in Fig. 3(a), are the E_u and A_{1g} modes. The SO effects cause the largest splitting of these two low optical modes at the Γ point. Again, the SO is significant to the dispersion of the E_u mode but not of the A_{1g} modes. Below these two modes in Fig. 3(a) are the $E_{g(a)}$ modes at 1.166 THz that correspond to another almost dispersionless branch in Fig. 3(b). As shown in Fig. 2, the difference between the $E_{g(a)}$ and $E_{g(b)}$ modes is that the top two layers vibrate in phase or out of phase. The frequency of the in-phase vibration is low, and the out-of-phase is high.

The phonon modes with the lowest frequency in the acoustic branches are the E_u and A_{2u} symmetry modes. When

waves propagate perpendicular to the QLs, the A_{2u} mode is a longitudinal mode and the E_u modes are two degenerate in-plane vibrations modes. These two E_u modes are sensitive to the external pressure, as discussed earlier.

All of the above features with and without SO are also true in Bi_2Te_3 bulk materials. But in bulk Bi_2Se_3 the $A_{2u(a)}$ mode is the third highest branch, and in bulk Bi_2Te_3 it is the fourth highest one. Because it makes a critical difference to include SO in calculations of phonon properties in the QL materials such as Bi_2Te_3 and Bi_2Se_3, in the results shown in this paper, SO is always included unless otherwise specified.

C. Phonon eigenmodes of single QL films with and without SO

Our calculated phonon dispersions for single QL films of Bi_2Te_3 and Bi_2Se_3 with and without SO are shown in Figs. 4 and 5; Fig. 4 is for the Bi_2Te_3 QL film, and Fig. 5 is for the Bi_2Se_3 QL film (the anharmonic potentials included in Figs. 4 and 5 will be discussed later). Comparing Figs. 4(a) and 4(b), we can see that, in general, the effects of SO to phonon dispersions of single QL films are similar to those of the bulk materials as discussed above. First, the frequencies with SO in Fig. 4(a) are lower than frequencies without SO in Fig. 4(b). For example, the highest frequency with SO of a Bi_2Te_3 single QL film is 4.092 THz, the highest frequency without SO of the same film is 4.176 THz, and the experimental measurement is 3.98 THz. We can also see in Fig. 4(a) that the dispersion of A modes at frequencies of ∼4.092, 3.973, 3.199, and 1.512 THz are less influenced by SO, comparing to the dispersion of E modes at frequencies of ∼2.87, 2.80, 1.57, and 0.90 THz. But in films, the E modes without SO are not as flat as in the bulk owing to the out-of plane vibrations in films, so the change of the dispersion in films with SO comparing to the dispersion without SO is not as noticeable as the corresponding bulk materials. We have also noticed the large difference between the A_{1g} mode and the E_u mode calculated with and without SO. All of these features exist in both single QL films and corresponding bulk materials.

In Fig. 5 we can see that all of the features that we have discussed in the results of Bi_2Te_3 QL films remain in the results of Bi_2Se_3 QL films.

One more topic we want to discuss here is the quantum confinement effects in films. Based on our previous understanding of phonons in nanocrystals,[36–38] by using a valence force field model, we know that the highest frequencies of nanosized structures will redshift from that of the bulk owing to the quantum confinement. This type of redshift sometimes can be used as a measure of the size of the nanomaterials. Based on this understanding, the quantum confinement should exist along the growth directions (c axis, or z direction) of the films. However, in our current calculations of first-principles approaches, this is not true for QL Bi_2Te_3 and Bi_2Se_3 films. The results in Table I show that the highest phonon frequencies of Bi_2Te_3 and Bi_2Se_3 single QL films are higher than the highest frequency of the corresponding bulk material when SO is included. Our understanding is that the effects of the change of crystal structures and force field near the surfaces were ignored in our previous investigations,[36–38] but are considered in the current first-principles approach. This tells us that when the material is very thin, such as the single QL, the effects of the change of crystal structures and force field should not be ignored. We have also noticed that in the Raman experimental measurement, the Raman-active highest-frequency modes of the Bi_2Te_3 and Bi_2Se_3 QL films have about the same frequency, or slightly higher frequency than those of the corresponding bulk materials, owing to the combination of the quantum confinement effect and the slight change of the crystals structures in these very thin films.

D. Phonon dispersion of the bulk Bi_2Te_3 under different pressures

One thing we noticed in our calculations is that the calculated phonon dispersions for both of the bulk materials and the films have some negative frequencies. The negative frequencies are related to the negative stress tensor of the optimized system. Because the GGA overestimates the lattice constants (the lattice constants calculated by both LDA and GGA are shown in Table I), the energy optimized structure has a negative stress tensor. Because the van der Waals interactions are weak in the z direction, the phonon modes in this direction are sensitive to the stress. So we can decrease the lattice constants slightly to obtain the positive acoustic branch, which is equivalent to increasing internal electronic pressure or external pressure. We used this method to investigate the effect of phonon dispersion of materials under pressure.

Because SO calculations are very time consuming, we first calculate pressure effects without SO, then we include SO to obtain accurate results. We found that the pressure effects with and without SO are similar. The calculated phonon dispersions of bulk Bi_2Te_3 under two different external pressures, 53 MPA and 2.066 GPA, both without SO, are shown in Fig. 6, and the results for Bi_2Se_3 are similar. The first external pressure of 53 MPA is the result of an energy-minimized structure and the second one of 2.066 GPA is the result of shrinking the lattice constants slightly and optimizing the energy again. For Bi_2Te_3, the lattice constants a and c shrank from 0.445 378 and 3.163 436 to 0.438 350 and 3.048 700, respectively (all in units of nm). As shown in Fig. 6, the two negative-frequency degenerated branches would become positive when the pressure increases. The VASP energy differences of the two Bi_2Te_3 structures with different electronic pressures in Fig. 6 are ∼0.07 eV, which is significant for van der Waals solids. In this process of increasing the pressure and thus decreasing the lattice constant, most of the phonon frequencies are increasing. From Fig. 6 we can see that some of the frequencies increase less, and those are modes with in-plane vibrations; some of the frequencies of the modes increase more, and those are modes with out-of-plane vibrations. This is easy to understand because of the van der Walls interaction between QLs in these systems. The fact that negative-frequency branches become positive with an external pressure suggests the phonon modes of the structure are strongly pressure dependent. The calculations show that van der Waals solids, such as Bi_2Te_3 and Bi_2Se_3, are similar to ferroelectric materials, and the phonon frequencies are sensitive to external pressures. Because the highest frequency for the optimized structures calculated by using GGA-PBE is close to the Raman experimental measurement,[15] we go ahead to calculate phonons of these energy optimized films.

E. Splitting of degenerate phonon modes at the Γ point owing to anharmonic potentials

In our calculations we found the existence of unusually strong anharmonic potentials in the growth directions around the Bi atoms in both of the Bi_2Te_3 and Bi_2Se_3 single QL films. These unusually strong anharmonic potentials cause the splitting of the phonon modes at the Γ point. To show our point more clearly, we show the results of phonon dispersion in single QL Bi_2Te_3 and Bi_2Se_3 films calculated without such anharmonic potentials in Fig. 7. In these calculations, the anharmonic potential obtained from the energy minimization is forcefully made harmonic. Comparing Fig. 4(a) with Fig. 7(a), we can see that the splitting of degenerated phonon modes at the γ point for Bi_2Te_3 films owing to the anharmonic potential can be clearly identified. In Fig. 4(a), where the anharmnoic potentials exist, these are $E_{u(b)}$ modes at 3.763 and 3.765 THz, $E_{g(b)}$ modes at 3.616 and 3.626 THz, $E_{u(a)}$ modes at 2.032 and 2.073 THz, and $E_{g(a)}$ modes at 1.15 and 1.173 THz (these values are listed in Table I); and in Fig. 7(a), where the potentials are forcefully made harmonic, all of these E modes are doubly degenerated. We can also see that the splitting is bigger for E modes in the lower-energy region and smaller for E modes in the higher-energy region. This kind of splitting for Bi_2Se_3 also exists but is smaller, as we can see from Figs. 5(a), 7(b), and Table I. These types of the anharmonic effects are also found to be strong for A modes, although there is nothing to split for the A modes, because A modes are modes with out-of-plane Bi vibrations in the z direction.

In our calculations, it is clearly shown that the VASP energy changes are different for the Bi atoms moving in the positive and negative z directions, but Se (or Te) atoms do not show this type of unsymmetrical and anharmonic effect. This anharmonic effect is mainly owing to the nonparabolic van der Waals potentials near the energy minimum. It is well known that thermal expansion of materials at finite temperature is an effect of the anharmonic potentials. Because almost all materials have thermal expansion at finite temperature, all of these materials have anharmonic potentials. However, we believe that Bi_2Te_3 and Bi_2Se_3 would have bigger thermal expansions than many other materials because of their strong anharmonic potentials. We think that this might be one of the reasons that Bi_2Te_3 and Bi_2Se_3 have a relatively low melting temperature.[15,16] In these van der Waals solids, the anharmonic interactions play an important role in the phonon properties. In general, we know that if the anharmonic potential is the same, the splitting will be smaller for systems with larger mass atoms, because the larger mass atoms have a larger inertia that is more difficult to change or to split their frequencies. However, this is not true when comparing Figs. 4 and 5, because Te is heavier than Se, but the splitting of Bi_2Te_3 is much bigger than Bi_2Se_3. Such anharmonic effects also exist in our calculations without SO, but they smaller. We believe that these anharmonic effects are partly from SO, because the SO of the heavier Te atom is stronger than that of the Se atom.

This unusual effect that SO is larger for heavier atoms is consistent with the SO-induced effects that we discussed earlier. The unique electronic structures including SO in these films provide unusual anharmonic potentials in these films, and we believe that this strong anharmonic potential is one of the major symmetry breakings in the quintuple films of Bi_2Te_3 and Bi_2Se_3 caused by SO. Our investigations of the electronic structures of single QL films will be published later.

F. Raman spectra in film and in bulk

Experimentally, it is observed that the phonon mode at 116.7 cm^{-1} (3.50 THz) is a Raman-active A_{2u} mode in Bi_2Te_3 (Ref. 16) (the definition of A_1 in Ref. 16 is the A_2 in MedeA), and it is also observed that the Raman intensity ratio of the highest-frequency A_{1g} modes to the intensity of the next Raman-active E_g mode increases as the thickness decreases, as reported in Fig. 3 of Ref. 16. From our calculated phonon dispersion of single quintuple Bi_2Te_3 and Bi_2Se_3 films, we understand this as the following: Because of the symmetry breaking in the films, the two top Raman-inactive A_{2u} modes in bulk become Raman active in thin films. In thin films, one of these two A_{2u} modes has a frequency close to the A_{1g} mode. Because experimentally it might be difficult to distinguish these two modes, the strengths of the Raman intensity of the highest-frequency A_{1g} modes increase as the thickness decreases, and this is in fact the combination of two Raman-active $(A_{1g} + A_{2u})$ modes, with an average frequency of 4.03 THz, as shown in the dispersion in Fig. 4 and Table I. Another Raman peak is from the second A_{2u} mode with a frequency of 3.2 THz (it is slightly different from the measured 3.5 THz in Ref. 16). This peak becomes Raman active in films, and it is a peak that does not exist in bulk.

IV. CONCLUSION

In this paper the phonon modes of single QL films of Bi_2Te_3 and Bi_2Se_3 and the corresponding bulk materials are calculated in detail. Phonon frequencies of bulk Bi_2Se_3 in LDA and GGA are compared. Phonon frequencies of bulk and films with and without SO are also compared. The SO effects on phonons in both bulk and films are discussed. It is shown that SO coupling adds another force field that lowers the frequencies in calculated results, which agree better with the experiments. The SO plays a very important role in the vibrations of E modes, which mainly vibrate within the films, and it plays a less important role in the vibration of A modes with only an out-of-plane component. A strong anharmonic potential is found to exist around Bi atoms in the single quintuple films, which is one of the symmetry breakings in these quintuple films caused by SO. From our calculated phonons of the Bi_2Te_3 and Bi_2Se_3 films, we can explain some of the features in Raman measurement of the materials. We can see that, owing to the symmetry breaking in the films, the two top Raman-inactive A_{2u} modes in bulk become Raman active in thin films. One of these two A_{2u} modes has a frequency close to the A_{1g} mode. Experimentally, it might be difficult to distinguish these two modes, so the measured strength of Raman intensity of the highest-frequency A_{1g} mode might be actually the combination of the two Raman-active $(A_{1g} + A_{2u})$ modes, so its strength increases as the thickness decreases. Another Raman peak is from the second A_{2u} mode in the films, which does not exist in bulk. These features are observed in the Raman measurement,[15,16,19,21,24] and are explained by our calculated results.

ACKNOWLEDGMENTS

The authors acknowledge the support of the subcontract of Dr. Y. Cui's KAUST Investigator Award (No. KUS-l1-001-12). They also acknowledge Dr. Y. Cui for suggesting this research topic and Dr. J. Cha and D. S. Kong for helpful discussions. Part of the work was performed when WC was a visitor at LBNL. The authors also acknowledge Professor D. S. Wang at the Institute of Physics (Beijing) for helpul discussions and his help in making the computation arrangement through his grant (NSFC-10634070). Part of the computation described in this research is carried out in the Supercomputing Center of Chinese Academy of Sciences in Beijing.

[1]H. J. Goldsmid and R. W. Douglas, Br. J. Appl. Phys. **5**, 458 (1954).
[2]A. F. Ioffe, *Semiconductor Thermoelectric and Thermoelectric Cooling* (Infosearch, London, 1957).
[3]D. A. Wright, Nature (London) **181**, 834 (1958).
[4]W. M. Yima and F. D. Rosi, Solid State Electron. **15**, 1121 (1972).
[5]S. K. Mishray, S. Satpathy, and O. Jepsen, J. Phys.: Condens. Matter **9**, 461 (1997).
[6]H. M. Cui, H. Liu, X. Li, J. Y. Wang, F. Han, X. D. Zhang, and R. I. Boughton, J. Solid State Chem. **177**, 4001 (2004).
[7]X. L. Li, K. F. Cai, H. Li, L. Wang, and C. W. Zhou, Int. J. Miner. Metall. Mater. **17**, 104 (2010)
[8]B. A. Bernevig, T. L. Hughes, and S. C. Zhang, Science **314**, 1757 (2006).
[9]M. Konig, S. Wiedmann, C. Brune, A. Roth, H. Buhmann, L. Molenkamp, X. L. Qi, and S. C. Zhang, Science **318**, 766 (2007).
[10]L. Fu and C. L. Kane, Phys. Rev. B **76**, 045302 (2007).
[11]H. Zhang, C. X. Liu, X. L. Qi, X. Dai, Z. Fang, and S. C. Zhang, Nat. Phys. **5**, 438 (2009).
[12]Y. Xia, D. Qian, D. Hsieh, L. Wray, A. Pal, H. Lin, A. Bansil, D. Grauer, Y. S. Hor, R. J. Cava, and M. Z. Hasan, Nat. Phys. **5**, 398 (2009).
[13]D. Hsieh, Y. Xia, D. Qian, L. Wray, J. H. Dil, F. Meier, J. Osterwalder, L. Patthey, J. G. Checkelsky, N. P. Ong, A. V. Fedorov, H. Lin, A. Bansil, D. Grauer, Y. S. Hor, R. J. Cava, and M. Z. Hasan, Nature (London) **460**, 1101 (2009).
[14]W. Y. Shan, H. Z. Lu, and S. Q. Shen, New J. Phys. **12**, 043048 (2010).
[15]D. Teweldebrhan, V. Goyal, and A. A. Balandin, Nano Lett. **10**, 1209 (2010).
[16]K. M. F. Shahil, M. Z. Hossain, D. Teweldebrhan, and A. A. Balandin, Appl. Phys. Lett. **96**, 153103 (2010).
[17]D. S. Kong, W. H. Dang, J. J. Cha, H. Li, S. Meister, H. L. Peng, Z. F. Liu, and Y. Cui, Nano Lett. **10**, 2245 (2010).
[18]S. S. Hong, W. Kundhikanjana, J. J. Cha, K. Lai, D. S. Kong, S. Meister, M. A. Kelly, Z. X. Shen, and Y. Cui, Nano Lett. **10**, 3118 (2010).
[19]V. Goyal, D. Teweldebrhan, and A. A. Balandin, Appl. Phys. Lett. **97**, 133117 (2010).
[20]D. Teweldebrhan, V. Goyal, M. Rahman, and A. A. Balandin, Appl. Phys. Lett. **96**, 053107 (2010).
[21]M. Z. Hossain, S. L. Rumyantsev, D. Teweldebrhan, K. M. F. Shahil, M. Shur, and A. A. Balandin, Phys. Status Solidi A **208**, 144 (2011).
[22]M. S. Dresselhaus, G. Chen, M. Y. Tang, R. G. Yang, H. Lee, D. Z. Wang, Z. F. Ren, J.-P. Fleurial, P. Gogna, Adv. Mater. **19**, 1043 (2007).
[23]L. D. Hicks and M. S. Dresselhaus, Phys. Rev. B **47**, 12727 (1993).
[24]W. H. Dang, H. L. Peng, H. Li, P. Wang, and Z. F. Liu, Nano Lett. **10**, 2870 (2010).
[25]MedeA is a trademark of Materials Design [http://www.materialsdesign.com].
[26]VASP stands for Vienna *ab initio* Simulation Package [http://cms.mpi.univie.ac.at/VASP/].
[27]W. Richter, H. Kohler, and C.R. Beker, Phys. Status Solidi **84**, 619 (1977).
[28]J. O. Jenkins, J. A. Rayne, and R. W. Ure Jr., Phys. Rev. B **5**, 3171 (1972).
[29]B. Qiu and X. Ruan, Phys. Rev. B **80**, 165203 (2009).
[30]J. P. Perdew and A. Zunger, Phys. Rev. B **23**, 5048 (1981).
[31]J. P. Perdew, J. A. Chevary, S. H. Vosko, K. A. Jackson, M. R. Pederson, D. J. Singh, and C. Fiolhais, Phys. Rev. B **46**, 6671 (1992).
[32]J. P. Perdew, J. A. Chevary, S. H. Vosko, K. A. Jackson, M. R. Pederson, D. J. Singh, and C. Fiolhais, Phys. Rev. B **48**, 4978 (1993).
[33]J. P. Perdew, K. Burke, and M. Ernzerhof, Phys. Rev. Lett. **77**, 3865 (1996).
[34]J. P. Perdew, K. Burke, and M. Ernzerhof, Phys. Rev. Lett. **78**, 1396 (1997).
[35]W. Cheng, L. Liu, P.Y. Yu, Z. X. Ma, and S. S. Mao, Ann. Phys. **523**, 129 (2011).
[36]W. Cheng, S. F. Ren, Phys. Rev. B **65**, 205305 (2002).
[37]S. F. Ren, W. Cheng, and P. Y. Yu, Phys. Rev. B **69**, 235327 (2004).
[38]W. Cheng, S. F. Ren, and P.Y. Yu, Phys. Rev. B **71**, 174305 (2005).